BioNanoScience
https://doi.org/10.1007/s12668-024-01478-x

RESEARCH

Development of Alginate and Chitosan Nanoparticles as Carriers of *Zingiber officinale* Essential Oil for Enhancement of Its Anticancer, Antibacterial, and Antifungal Activities

Elham Zarenezhad[1] · Mohammad Hosein Afsarian[2] · Hiva Alipanah[3] · Fatemeh Yarian[4] · Hamid Moradi[5] · Houssam-Eddin Khalaf[6] · Mahmoud Osanloo[7]

Accepted: 27 May 2024

Abstract

The rise of drug resistance has led to attempts to the development of new herbal medicines. This study aimed to develop two types of nanocarriers containing *Zingiber officinale* essential oil. The oil's components were identified using GC-MS analysis. Alginate and chitosan nanoparticles containing *Z. officinale* essential oil were prepared using the ionic gelation method. Particle size, zeta potential, and successful loading of the essential oil in the nanoparticles were investigated using DLS, Zetasizer, and ATR-FTIR analysis, respectively. Chitosan nanoparticles exhibited a significantly smaller particle size (102 ± 9 nm) and more positive zeta potential (12 ± 2 mV) compared to alginate counterparts (188 ± 7 nm, -19 ± 1.2 mV). ATR-FTIR analysis confirmed the successful encapsulation in both types of nanoparticles. Notably, chitosan nanoparticles with IC_{50} values of 82 and 67 µg/mL against MCF-7 and MDA-MB-231, respectively, displayed superior potency compared to non-formulated essential oil and alginate nanoparticles. Likewise, the antibacterial efficacy of chitosan nanoparticles with IC_{50} values of 661 and 462 µg/mL against *Escherichia coli* and *Staphylococcus aureus*, respectively, showed a significant potency compared to two other samples. Furthermore, chitosan nanoparticles demonstrated antifungal activity against *Candida krusei* (MIC 4.25 µg/mL) and *Candida parapsilosis* (MIC 8.5 µg/mL) while showing no significant antifungal activity against *Aspergillus flavus* (MIC > 1200). Considering their high potency and straightforward preparation, chitosan nanoparticles loaded with *Z. officinale* essential oil warrant further investigation in vivo.

Keywords Nanotechnology · Breast cancer · Bacteria · Fungal infections · Herbal medicine

✉ Mahmoud Osanloo
osanloo_mahmood@yahoo.com; m.osanloo@fums.ac.ir

1 Noncommunicable Diseases Research Center, Fasa University of Medical Sciences, Fasa, Iran

2 Department of Parasitology and Mycology, School of Medicine, Fasa University of Medical Sciences, Fasa, Iran

3 Department of Physiology, School of Medicine, Fasa University of Medical Sciences, Fasa, Iran

4 Department of Medical Biotechnology, School of Advanced Technologies in Medicine, Fasa University of Medical Sciences, Fasa, Iran

5 Student Research Committee, Fasa University of Medical Sciences, Fasa, Iran

6 Division of Molecular Biomedicine, Department of Molecular Biology and Biotechnology, Atomic Energy Commission of Syria (AECS), Damascus, Syria

7 Department of Medical Nanotechnology, School of Advanced Technologies in Medicine, Fasa University of Medical Sciences, Fasa, Iran

1 Introduction

Drug resistance is a major challenge for healthcare systems worldwide. Medicinal plants are a valuable resource for developing new drugs [1, 2]. For instance, *Zingiber officinale* (ginger) belongs to the Zingiberaceae family and has been a widely used medicinal plant. It is grown in moist, tropical, subtropical regions [3, 4]. Its essential oil (EO) has been used in colds, nausea, emesis, and headaches [5, 6]. *Z. officinale* also showed anti-inflammatory, antioxidant, anticancer, antimicrobial, and anti-diabetic activities [7, 8]. Researchers demonstrated that the aqua-alcoholic extract of *Z. officinale* as an effective agent inhibited the growth of a multidrug-resistant strain of *Pseudomonas aeruginosa* [9]. In addition, a study showed that *Z. officinale* extract inhibits biofilm formation through reduced cellular c-di-GMP in *P. aeruginosa* [10]. *Pseudomonas aeruginosa* is a gram-negative bacteria that can cause various human infections,

Published online: 04 June 2024

such as the skin, lungs, and urinary tract, increasing mortality rates [11]. Moreover, its ethanol extracts could act as a potent antibiotic agent against *Staphylococcus aureus*, a gram-positive human pathogen bacteria that can cause a wide range of clinical diseases [12]. In vitro antibacterial activity showed that *Z. officinale* inhibited *S. aureus* due to inhibiting the activity of 6-hydroxymethyl-7,8-dihydropterin pyrophosphokinase in the pathogen [13]. Moreover, *Candida* is a kind of yeast that is the most common cause of fungal infections worldwide [14]. The genus *Candida* enfolds approximately 200 species, such as *C. albicans*, *C. glabrata*, C. *rugosa*, *C. parapsilosis*, *C. tropicalis*, and *C. dubliniensis* [15, 16]. Recently, it was reported that *Z. officinale* EO displayed antifungal activity toward *C. albicans* [17]. Another study confirmed that *Z. officinale* extract potently treats oral candidiasis [18]. Regarding the antibacterial and antifungal activities of *Z. officinale*, some studies have also shown its anticancer activity against several cancer types, including prostate, breast, colorectal, and cervical cancer [19, 20]. In vivo study in mice demonstrated that *Z. officinale* extract protected against breast cancer via activation of 5′adenosine monophosphate–activated protein kinase (AMPK) and the downregulation of cyclin D1 [20]. Breast cancer, with 2.26 million cases and 685,000 deaths in 2020, was one of the most dangerous cancers worldwide [21]. *Z. officinale*'s EO exhibits diverse biological properties, but developing a standardized drug faces three hurdles: poor solubility and bioavailability, limited efficacy, and short shelf life. Encapsulating the EO in nanocarriers holds promise to overcome these challenges [22]. Natural polymeric nanoparticles such as chitosan and alginates have attracted interest in drug delivery systems due to their biocompatibility, biodegradability, and low cytotoxicity [23, 24].

This study attempted to enhance the efficacy of *Z. officinale* EO by preparing chitosan and alginate nanoparticles containing the EO. Their particle size and zeta potential were compared. Successful loading of the EO in chitosan and alginate nanoparticles was investigated. Their antimicrobial, antifungal, and anticancer activities were also compared.

2 Materials and Methods

2.1 Materials

Zingiber officinale Roscoe EO was bought from Zardband Pharmaceuticals Co. (Iran). *Staphylococcus aureus* (ATCC 25,923), *Escherichia coli* (ATCC 25,922), MCF-7 (ATCC: HTB-22), and MDA-MB-231 (ATCC: HTB-26) were purchased for the Pasteur Institute of Iran. Itraconazole was obtained from the Janssen Research Foundation, Beerse, Belgium, and fluconazole from Pfizer, Groton, CT, USA. Standard fungi isolates containing *Candida krusei* (ATCC 6258), *Candida parapsilosis* (ATCC22019), and *Aspergillus flavus* (ATCC 204,304) were obtained from collections of ATCC (American Type Culture Collection). M-morpholine propane sulfonic acid (MOPS) buffer was supplied from Merck Chemicals (Germany). L-Glutamine and tripolyphosphate (TPP) were bought from Sigma-Aldrich (USA).

2.2 Chemical Composition of *Z. officinale* EO

The phytochemical compounds of EO were identified using an Agilent GC-MS (Santa Clara, CA, USA) system with a BPX5 silica fused column (film thicknesses 0.25 mm, length 30 m, and internal diameter 0.25 µm). The EO is diluted with *n*-hexane, and the sample was injected into the GC-MS. Initially, the oven temperature was held at 50 °C (fixed for 5 min), then increased with a rate of 3 °C min^{-1} to 240 °C. The temperature was then raised to 300 °C and held for 3 min at this temperature, and the response time was 52 min. The temperature of the injection port was fixed at 250 °C, in split 1 to 35. The flow rate of helium (99.999%) as carrier gas was 0. 5 mL/min. For MS spectra, the ionization conditions were full scan mode in 30–500 m/z, electron energy of 70 eV, and ion source temperature of 220 °C. For spectra analysis, Agilent ChemStation software was used. Finally, the final spectra identified compare chemical compounds' spectral data and retention index using papers, reference books, and the mass spectra of standard compounds.

2.3 Preparation of Alginate and Chitosan Nanoparticles Containing *Z. officinale* EO

The ionic gelation method was used to prepare alginate and chitosan nanoparticles containing *Z. officinale* EO. $CaCl_2$ (0.03% w/v) and TPP (0.07% w/v) were used as their crosslinkers, respectively [25, 26]. Fixed amounts of *Z. officinale* EO (0.24% w/v) and Tween 20 (0.15% w/v) were considered for both nanoformulations.

Alginate (0.25% w/v) and chitosan (0.25% w/v) powders were dissolved in acid acetic (1% w/v) and distilled water stirred overnight at 2000 rpm. After that, the obtained solutions were filtered using 0.2 µm, and the preparation process was continued as follows. The EO and Tween 20 were mixed at 2000 rpm for 3 min; then, chitosan and alginate solution were added, dropped wisely, and stirred for 5 min, separately. Afterward, $CaCl_2$ and TPP were added and stirred for 40 min for crosslinking and stabilizing. The formed alginate and chitosan nanoparticles containing *Z. officinale* EO were named AlginateNPs-EO and ChitosanNPs-EO. By the way, nanoparticles without EO were prepared similarly and were named Alginate-Free and Chitosan-Free; their biological effects were investigated as negative control groups.

2.4 Characterizations of AlginateNPs-EO and ChitosanNPs-EO

Particle size, polydispersity index (PDI), and zeta potentials of Alginate-Free, AlginateNPs-EO, Chitosan-Free, and ChitosanNPs-EO were investigated using a DLS-type apparatus (Horiba, SZ100, Japan). ATR-FTIR analysis was used to investigate the successful loading of the EO in the nanoparticles. Spectra of *Z. officinale* EO, Alginate-Free, AlginateNPs-EO, Chitosan-Free, and ChitosanNPs-EO were recorded in the 400–4000 cm^{-1} range.

2.5 Antifungal Effects of *Z. officinale* EO, AlginateNPs-EO, and ChitosanNPs-EO

The samples' minimal inhibitory concentrations (MICs) were determined by the micro broth dilution method in 96-well microplates due to the CLSI-M27-A3 and M27-S4 methods for fungi [27, 28]. Itraconazole and fluconazole were used as the positive control. The samples were serially diluted in the standard RPMI-1640 medium and buffered to pH 7.0 with 0.165 M-morpholine propane sulfonic acid (MOPS) buffer and L-glutamine without bicarbonate. Meanwhile, suspended colonies were added to microplates and incubated at 35 °C. All susceptibility testing was repeated in triplicates.

2.6 Antibacterial Effect of *Z. officinale* EO, AlginateNPs-EO, and ChitosanNPs-EO

The microdilution method in a 96-well plate was used to determine the antibacterial effect of samples against *S. aureus* and *E. coli* [29]. Suspended colonies in Mueller Hinton broth with 0.5 McFarland turbidity (1.5×10^8 CFU/mL) and serial dilutions of samples (dissolved in PBS solution) were added to plates (50:50 µL/well). By the way, 50 µL/well of PBS solution (as control group) and 50 µL/well of Alginate-Free and Chitosan-Free (as negative control groups) were added to the plates instead of serial dilutions. After 24 h incubation, bacterial growth was calculated by dividing the optical density of samples to control at 630 nm using the plate reader. The test was repeated thrice, and the results are reported as mean and standard deviation. Besides, IC_{50} values of samples were calculated using CalcuSyn software (Free version, BIOSOFT, UK).

2.7 Investigation of Cytotoxic Effects of *Z. officinale* EO, AlginateNPs-EO, and ChitosanNPs-EO

As described in our previous study, the MTT assay was used to investigate the cytotoxic effects of samples against MCF-7 and MDA-MB-231 cells [30]. The cells were cultured in RPMI perfect medium culture (supplemented with 10% FBS and 1% antibiotics); 10^4 cells/well seeded in 96-well plates. The plates incubated for 24 h at 37 °C and 5% CO_2 to the attachments reached 80% confluence. The liquid medium of the plates was then discarded. After that, 50 and 50 µL/well of fresh RPMI perfect medium culture and serial dilutions (dissolved in PBS solution) were added. By the way, 50 µL/well of PBS solution (as control group) and 50 µL/well of Alginate-Free and Chitosan-Free (as negative control groups) were added to the plates instead of serial dilutions. After 24 h incubation, liquid medium was replaced with 50 µL/well of MTT solution (0.5 mg/mL dissolved in RPMI). After 4 h incubation, 100 µL/well of DMSO was added to dissolve formazan crystals. After that, cell viability was calculated by dividing the optical density of samples to control at 570 nm using a plate reader (Synergy HTX Multi-Mode Reader, USA). The test was repeated thrice, and the results are reported as mean and standard deviation. Besides, IC_{50} values of samples were calculated using CalcuSyn software (Free version, BIOSOFT, UK).

3 Results

Identified compounds in *Z. officinale* EO are listed in Table 1. Zingiberene, β-sesquiphellandrene, α-curcumene, β-bisabolene, and camphene are five major components.

DLS diagrams of the prepared samples are depicted in Fig. 1. The particle size of Alginate-Free, AlginateNPs-EO, Chitosan-Free, and ChitosanNPs-EO were obtained as 166 ± 8, 188 ± 7, 77 ± 5, and 102 ± 9 nm. Besides, their PDI values were obtained as 0.6, 0.2, 0.4, and 0.3. Furthermore, zeta potential profiles of the samples, including Alginate-Free (-16 ± 1 mV), AlginateNPs-EO (-19 ± 1.2 mV), Chitosan-Free (17 ± 0.9 mV), and ChitosanNPs-EO (12 ± 2 mV) are shown in Fig. 2.

The ATR-FTIR spectrum of *Z. officinale* EO (Fig. 3(A)) showed that the peaks at 3077 and 3021 cm^{-1} are related to the stretching vibration of =C-H. The bands at 2959, 2923, and 2870 cm^{-1} displayed the CH stretching vibration of sp^3 in alkanes. The characteristic band at 1722 and 1673 cm^{-1} is allocated to EO's carbonyl group stretching vibration. The bands at 1514 and 1450 cm^{-1} showed the C=C vibration of aromatic compounds in EO. The strong band at 985 cm^{-1} corresponded to C-O stretching vibration.

ATR-FTIR spectrum of Alginate-Free is shown in Fig. 3(B). The stretching vibration of the O-H peak of alginate is shown at 3200–3600 cm^{-1} due to hydrogen bonding, and the bands at 2913 and 2884 cm^{-1} can be related to C-H (stretching vibration). The spectra at 1731 cm^{-1} can correspond to the carbonyl group's stretching vibration. The characteristic spectra at about 1595 and 1406 cm^{-1} were attributed to carboxylate's asymmetric and symmetric

Table 1 Identified compounds in *Z. officinale* EO using GC-MS analysis

Retention time	Compound	Area	%	Retention index
9.46	α-Pinene	136,969,687	2.408	932
10.109	Camphene	383,028,771	6.735	954
13.687	1,8-Cineole	173,585,602	3.052	1026
13.784	β-Phellandrene	313,546,839	5.513	1029
20.12	Borneol	67,785,724	1.192	1169
30.111	β-Elemene	61,307,533	1.078	1390
33.997	α-Curcumene	660,313,772	11.611	1480
34.703	Zingiberene	1,722,333,976	30.285	1493
35.07	β-Bisabolene	607,823,161	10.688	1505
35.728	β-Sesquiphellandrene	703,494,850	12.370	1522

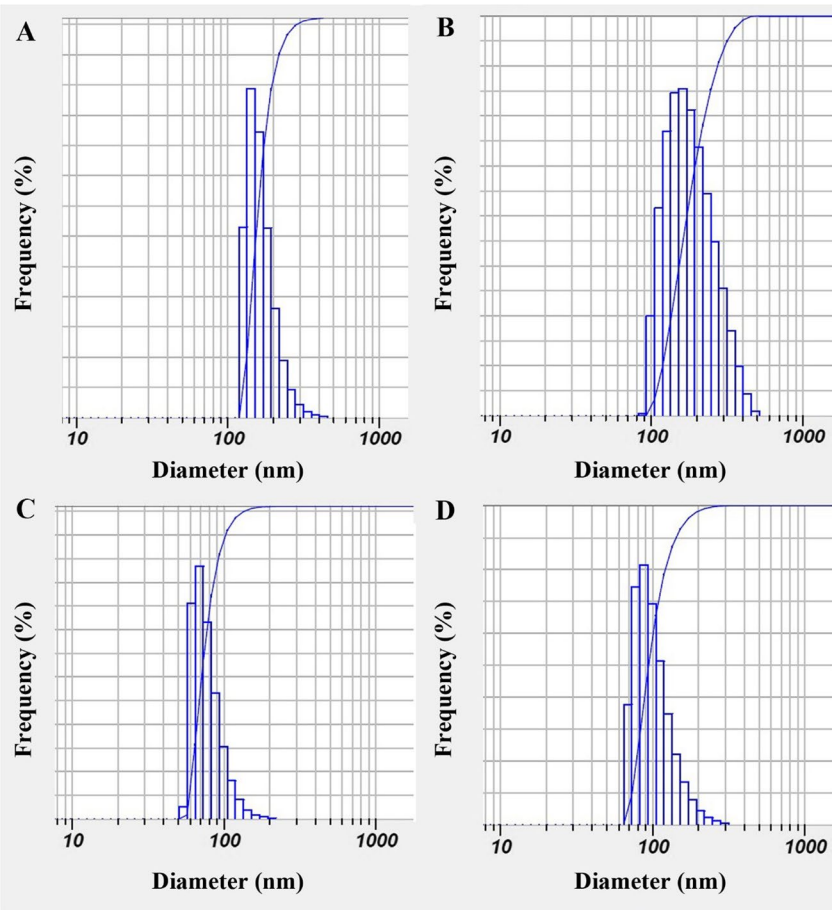

Fig. 1 DLS diagrams of **A** Alginate-Free (166 8 nm, PDI 0.6), **B** AlginateNPs-EO (188 7 nm, PDI 0.2), **C** Chitosan-Free (77 5 nm, PDI 0.4), **D** ChitosanNPs-EO (102 9 nm, PDI 0.3)

stretching vibration, and the peaks at 1066 and 1028 cm^{-1} were allocated to C-O stretching vibration.

ATR-FTIR spectrum of AlginateNPs-EO is shown in Fig. 3(C). The broad peak at about 3200–3600 cm^{-1} is attributed to OH vibration due to hydrogen bonding in Tween 20, EO, water, and alginate. The peaks displayed at 3197 and 3040 cm^{-1} can be related to C = C-H stretching, and the peaks at 2925 and 2857 cm^{-1} are allocated to CH_2 stretching vibration. The absorption at 1731 cm^{-1} can be allocated to the stretching vibration of the carbonyl group in Tween and EO. The bands at 1531 and 1461 cm^{-1} can be allocated to carboxylate's asymmetric and symmetric stretching vibration. The 1352 and 1034 cm^{-1} peaks can be related to C-O stretching vibration. The bands shift to lower wavenumbers are shown by the increase in hydrogen bonding. The strong spectra at 1095 cm^{-1} can correspond to the reaction between the calcium ion and carboxyl (CO-Ca-CO group structure), which enhanced C-O vibration. These spectra illustrated ionic crosslinking. The presence of other spectra in alginate nanoparticles and EO

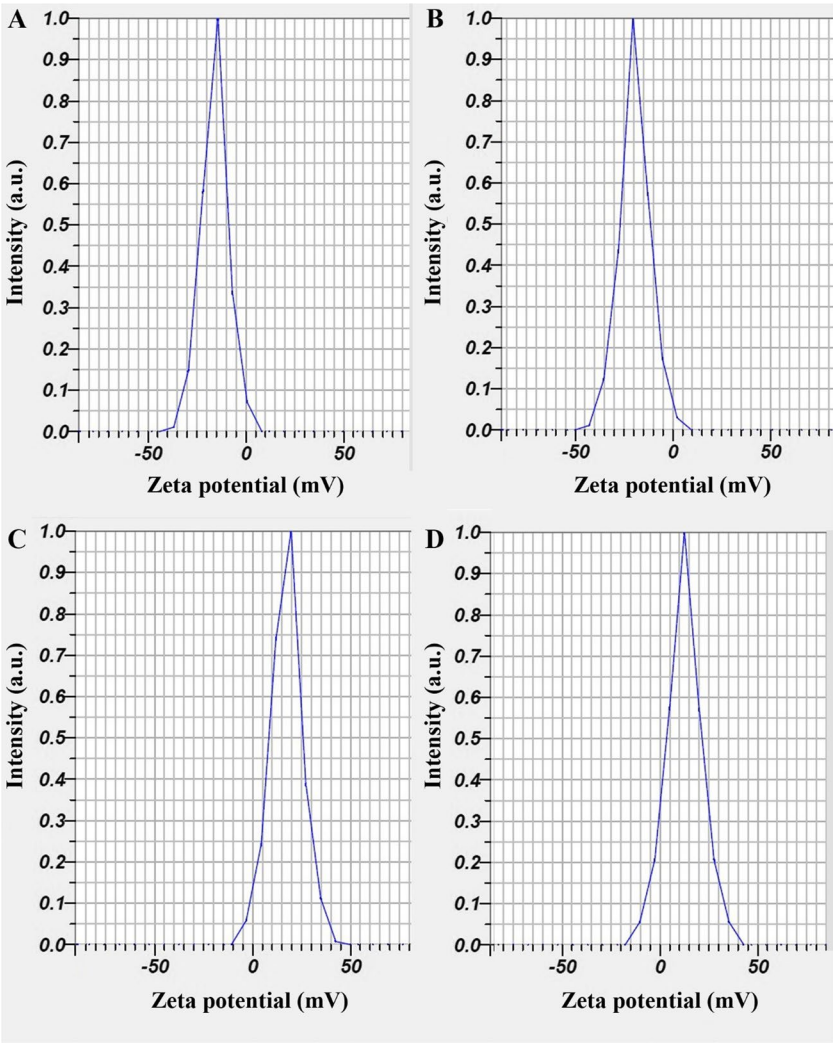

Fig. 2 Zeta potential diagrams of **A** Alginate-Free (−16 1 mV), **B** AlginateNPs-EO (−19 1.2 mV), **C** Chitosan-Free (17 0.9 mV), **D** ChitosanNPs-EO (12 2 mV)

confirmed the successful loading of EOs in the prepared alginate nanoparticles.

The ATR-FTIR spectrum of Chitosan-Free (Fig. 3(D)) showed that the broadband between 3300 and 36,684 cm^{-1} can be attributed to the stretching vibration of the hydroxyl group due to hydrogen bonding. The spectra at 2970 cm^{-1} can be related to the stretching vibration of CH in sp^3 groups. The strong band at 1731 cm^{-1} can be allocated to the carbonyl group. The characteristic band at 1639 cm $^{-1}$ can be related to *N*-acetyl groups. The band at 1549 cm^{-1} can be assigned to N-H bending vibration, and the band at 1279 cm^{-1} demonstrated the presence of P = O. The band at 1078 cm^{-1} and 1019 can be attributed to the stretching vibration of PO_2 and PO_3. The band at 889 cm^{-1} is related to the P-O-P bridge.

The ATR-FTIR spectrum of ChitosanNPs-EO (Fig. 3(E)) showed that the broad and characteristic peak between 3325 and 3684 cm^{-1} can be related to OH stretching vibration due to hydrogen bonding. The band at 2985 cm^{-1} is ascribed to the stretching vibration of CH in alkane groups. The strong and characteristic spectra at 1711 cm^{-1} can be assigned to the carbonyl group. The spectra at 1549 cm^{-1} can be attributed to N-H bending vibration. The spectra at 1278 cm^{-1} illustrated the formation of an ionic crosslink between NH_3 in chitosan and TPP. The strong peaks at 1077 and 1019 cm^{-1} can be related to the stretching vibration of PO_2 and PO_3. The band at 889 cm^{-1} is related to the P-O-P bridge. All other absorption appears in the spectra of EO and ChiNPs at the same wavenumber.

The antifungal activity of *Z. officinale* EO, AlginateNPs-EO, ChitosanNPs-EO, and itraconazole and fluconazole against *C. krusei*, *C. parapsilosis*, and *A. flavus* are shown in Table 2. The lowest MIC is related to ChitosanNPs-EO: 4.25 µg/mL for *C. krusei* and 8.5 µg/mL for *C. parapsilosis*. Besides, ChitosanNPs-EO against *A. flavus* displayed the MIC with > 1200 µg/mL. The in vitro MIC results obtained for itraconazole and fluconazole against the standard tested isolates were within the normal ranges for these strains [31].

The antibacterial effects of *Z. officinale* EO, AlginateNPs-EO, and ChitosanNPs-EO against *E. coli* and *S. aureus* are

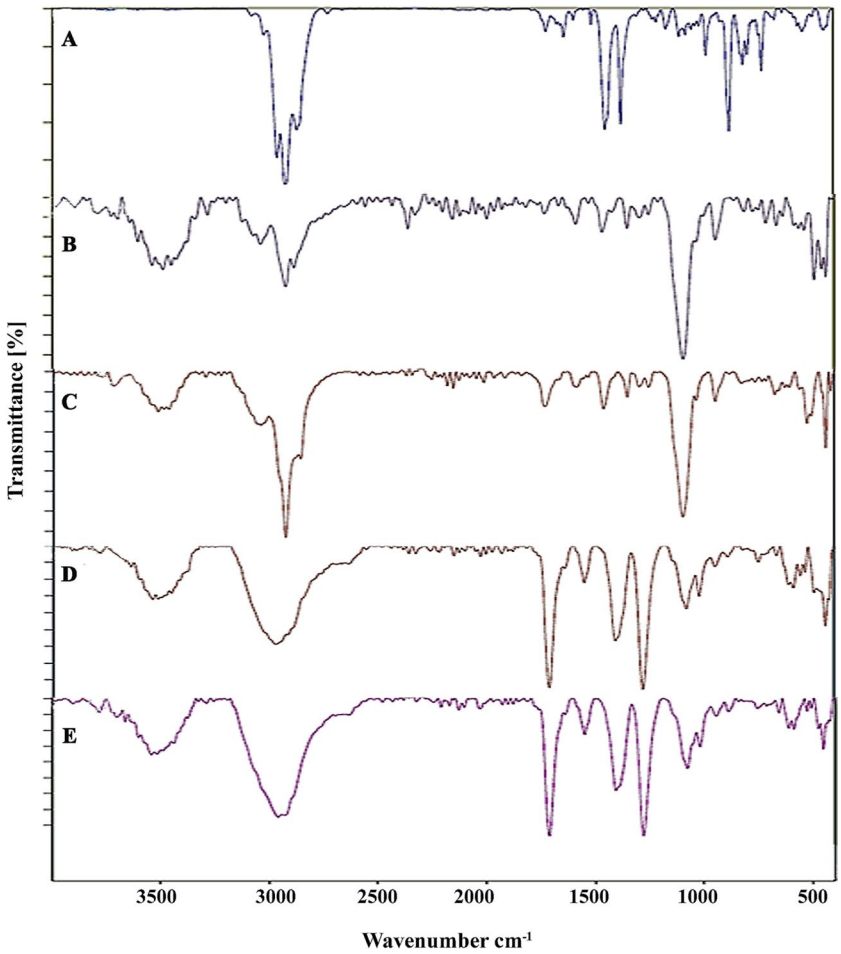

Fig. 3 ATR-FTIR spectra of (**A**) Z. officinale EO, (**B**) Alginate-Free, (**C**) AlginateNPs-EO, (**D**) Chitosan-Free, (**E**) ChitosanNPs-EO

Table 2 Obtained MIC values of *Z. officinale* EO, AlginateNPs-EO, ChitosanNPs-EO, and itraconazole and fluconazole

Samples	MIC (µg/mL)		
	C. krusei	*C. parapsilosis*	*A. flavus*
Z. officinale EO	> 1200	> 1200	> 1200
AlginateNPs-EO	> 1200	> 1200	> 1200
ChitosanNPs-EO	4.25	8.5	> 1200
Itraconazole	0.125	0.125	0. 25
Fluconazole	64	0.25	2

shown in Fig. 4A, B. The best efficacy is related to ChitosanNPs-EO; the growth of bacteria was reduced by about 60%. Besides, Alginate-Free and Chitosan-Free did not affect bacterial growth. Moreover, IC_{50} values of the samples against bacteria are summarized in Table 3. ChitosanNPs-EO with IC_{50} values of 661 and 462 µg/mL against *E. coli* and *S. aureus*, respectively, were significantly more potent than *Z. officinale* EO and AlginateNPs-EO. Their IC_{50} values against *E. coli* were 9537 and 2050 µg/mL, respectively. Besides, their IC_{50} values against *S. aureus* were obtained as 5486 and 1473 µg/mL, respectively.

Cytotoxicity of *Z. officinale* EO, AlginateNPs-EO, and ChitosanNPs-EO against MCF-7 and MDA-MB-231 cells are shown in Fig. 5A, B. Interestingly, 100% efficacy (cell viability 0%) at concentrations of 600 and 1200 µg/mL of ChitosanNPs-EO were observed. On the other hand, Alginate-Free and Chitosan-Free showed negligible effects on the viability of cells (viability > 90%). Moreover, IC_{50} values of the samples against cells are summarized in Table 3. ChitosanNPs-EO with IC_{50} values of 82 and 67 µg/mL against MCF-7 and MDA-MB-231 cells, respectively, were significantly more potent than *Z. officinale* EO and AlginateNPs-EO. IC_{50} values of *Z. officinale* EO against MCF-7 and MDA-MB-231 cells were 699 and 566 µg/mL, respectively, and these values for AlginateNPs-EO were 590 and 218 µg/mL, respectively.

4 Discussion

In recent years, in vitro and in vivo studies indicate a wide range of bioactivities of natural products, especially antimicrobial and anticancer activities [32, 33]. Nowadays, phytomedicine researchers focus on applied research to develop

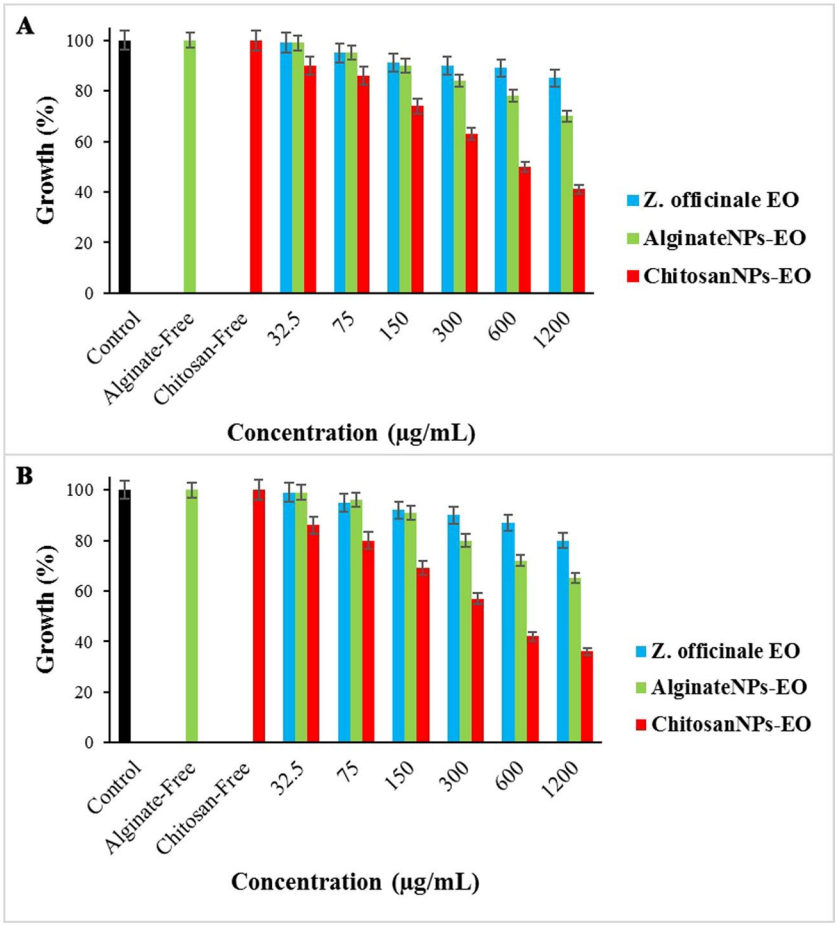

Fig. 4 Bacterial growth after treatment with *Z. officinale* EO, AlginateNPs-EO, and Chitosan-NPs-EO against **A** *E. coli* and **B** *S. aureus*

Table 3 Obtained IC 50 values of Z. officinale EO, AlginateNPs-EO, and ChitosanNPs-EO

Samples	Parameter	MCF-7	MDA-MB-231	*E. coli*	*S. aureus*
Z. officinale EO	IC_{50}	699	566	9537	5484
	LCL	244	348	1312	1589
	UCL	2002	921	69,320	18,931
AlginateNPs-EO	IC_{50}	590	218	2050	1473
	LCL	190	191	1010	910
	UCL	1833	248	4158	2386
ChitosanNPs-EO	IC_{50}	82	67	661	462
	LCL	37	30	554	401
	UCL	183	149	789	532

new drugs based on nano-based drug delivery systems. This study investigated chitosan and alginate nanoparticles containing *Z. officinale* EO as a model drug delivery system for their effects on fungal and bacterial growth and breast cancer cell viability.

A. flavus is a fungal species that can cause various health challenges. Sensitization was diagnosed through positive immunological tests [34]. *A. flavus* is also known for its ability to produce aflatoxins, which are highly carcinogenic mycotoxins. Also, *C. krusei* is a species of *Candida* that has gained importance in recent years as a cause of candidiasis, particularly in immunocompromised patients [35, 36]. The main challenges in treating *C. krusei* infections include its ability to develop resistance to antifungal drugs and evade the host's immunity [37]. Studies have shown that *C. krusei* is resistant to fluconazole and other antifungal drugs [38, 39]. The incidence of *C. krusei* infections has been increasing, highlighting the need for effective treatment strategies. Several studies have also highlighted the prevalence and antifungal susceptibility of *C. parapsilosis* in different

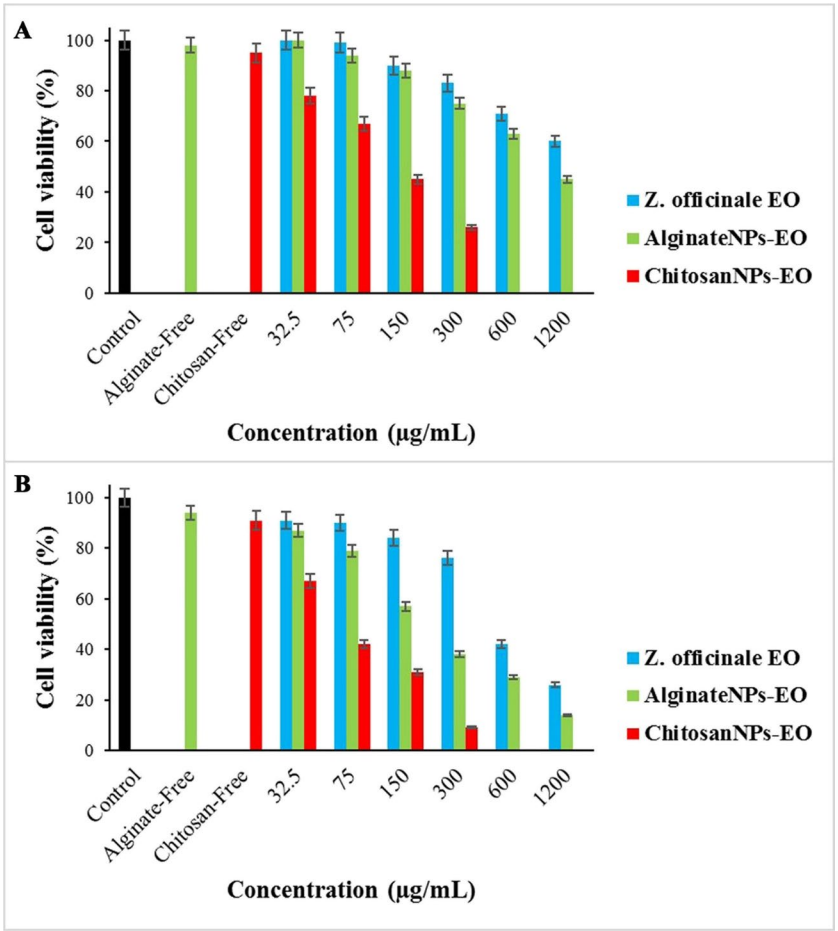

Fig. 5 Cytotoxicity of *Z. officinale* EO, AlginateNPs-EO, and ChitosanNPs-EO against **A** MCF-7 and **B** MDA-MB-231 cells

countries [40, 41]. The prevalence of *C. parapsilosis* has been associated with clinical settings, such as patients with cancer or cardiovascular diseases [42]. Additionally, *C. parapsilosis* candidemia has been associated with lower mortality rates than *C. albicans* candidemia [43]. Interestingly, ChitosanNPs-EO in the current study showed promising effects on three examined fungi. *Z. officinale* Roscoe EO, as noted by Samuel et al., was capable of inhibiting growth and aflatoxin production in *A. flavus* [44]. This result confirms the previously published reports demonstrating that *Z. officinale* Roscoe EO inhibits the growth and aflatoxin production of *A. flavus* [45–47]. It has also been shown that *Z. officinale* (concentrations between 0.625 and 5 mg/mL) can inhibit biofilm formation by *C. krusei* and *C. albicans* [48]. These data are congruent with the results of other reports demonstrating that *Z. officinale* had an inhibitory effect on *C. albicans* [49]. There have been no studies on the antifungal effect of alginate and chitosan nanoparticles as carriers of Z. *officinale* EO on *A. flavus*, *C. krusei*, and *C. parapsilosis*; our findings indicated that chitosan nanoparticles had a more significant antifungal compare with alginate nanoparticles. In agreement with our findings, it has been suggested that treatment with chitosan, a natural antifungal agent, reduced the growth and aflatoxin production of certain *A. flavus* strains [50]. Also, the antifungal activity of copper-chitosan nanocomposite hydrogels against *A. flavus* was reported to have decreased aflatoxin-producing ability [51]. This finding coincided with a study that demonstrated MIC_{90} in chitosan solution was more than nanoparticles for the selected fungi species and concluded that nanoformulation increased chitosan antifungal activity [52]. Previous studies also showed that alginate-based carriers can improve antifungal drugs' bioavailability and dosing frequency [53]. For example, the antioxidant and antimicrobial activities of alginate microparticles containing *Satureja hortensis* EO were investigated; results showed that alginate microparticles could be used as an antioxidant and antimicrobial agent with a controlled release manner [54]. In addition, encapsulation of clove, thyme, and cinnamon oils in alginate microspheres can prolong antifungal activity by reducing evaporation of EOs [55].

Another finding has been spotted in our study: remarkably reduced (≈40%) *E. coli* and *S. aureus* growth in the ChitosanNPs-EO (1200 µg/mL)-treated bacteria. Emerging evidence suggests that chitosan nanoparticles of EOs increase broad-spectrum antibacterial activities. For example,

chitosan nanoparticles loaded with clove EO against *Listeria monocytogenes* and *S. aureus* showed better antibacterial activity than clove EO [56]. In addition to the antibacterial properties of chitosan nanoparticles confirmed by previous studies, it can be assumed that chitosan nanoparticles containing EO can trigger cell death by penetrating the bacterial cell membrane and changing the balance of internal osmolarity [57, 58].

In our study, GC-MS analysis showed that the main chemical composition of *Z. officinale* EO was zingiberene (30.28%). It has been shown that exposure to zingiberene can reduce cell viability in the MDA-MB-231 breast cancer cell line by a significant increase in apoptotic cell death [59]. Like breast cancer, zingiberene suppressed colon cancer cell growth by inducing autophagy and inhibiting cell signaling (PI3K/AKT/mTOR and caspase 2) pathways [60]. As well as the antibacterial activity of zingiberene against *Streptococcus mutans UA159* in biofilm formation was confirmed [61].

In addition to the anticancer properties of EOs and their main compounds, many studies have shown that nanoformulation can dramatically increase the pharmacological and biological activities of EOs. For example, the *Z. officinale* EO was encapsulated in chitosan nanoparticles, improving its stability, solubility, antioxidant, and antibacterial properties [62]. Also, nanoemulsions containing *Z. officinale* extract had a potent ability to scavenge DPPH (2,2-diphenyl-1-picrylhydrazyl) and ABTS (2,2-azino-bis-3-ethylbenzothiazoline-6-sulfonic acid) free radicals, as well as had a toxicity effect against PC3 cancer cells [63]. Our data also indicated that the anticancer activity of nanoformulations of *Z. officinale* EO was more potent than non-formulated states on MDA-MB-231 and MCF-7 cell lines. It is important to note that ChitosanNPs-EO had more significant anticancer effects than AlginateNPs-EO. As well as, both nanoparticles induced 100% mortality in both cell lines at a concentration of 600 µg/mL, which confirmed the dose-dependent activity of nanoparticles. AlginateNPs-EO and ChitosanNPs-EO of *Zingiber officinale* EO reduced the MDA-MB-231 cell line by about 80% at 300 and 1200 µg/mL concentrations, respectively.

The IC_{50} of ChitosanNPs-EO for MDA-MB-231 and MCF-7 cell lines were 67 and 82 µg/mL, respectively. Alginate-based drug carriers could also reduce MDA-MB-231 and MCF-7 cell proliferation. Still, the IC_{50} of AlginateNPs-EO (MDA-MB-231, 218 µg/mL; MCF-7, 590 µg/mL) was higher than IC_{50} of ChitosanNPs-EO and demonstrated almost similar values with EO-treated cells. There is a confirmed improvement in the anticancer effect of ChitosanNPs-EO compared to AlginateNPs-EO and *Z. officinale* EO. These findings are congruent with other studies that reported a significant increase in the anticancer activity of loaded nanoparticles compared to free agents. For example, a report explored the incorporation of *Zataria multiflora* EO into chitosan biopolymer nanoparticles to improve its in vitro anticancer efficacy and conducted that treatment with NPs could alleviate the proliferation rate of breast cancer cells more than *Z. multiflora* EO [64]. In addition, the results of an in vitro cytotoxicity study on Hep-G2 (human liver cancer cell line) revealed that chitosan nanoparticles loaded by *Boswellia sacra* EO could upregulate apoptosis genes and reduce cancer cell migration and angiogenesis [65]. In addition, alginate nanoparticles containing *Syzygium aromaticum* EO caused cancer cell death, confirmed by an increase in the Bax/BCl-2 (apoptotic genes) ratio [66].

5 Conclusion

AlginateNPs-EO and ChitosanNPs-EO were successfully prepared and characterized. Results showed higher antifungal, antibacterial, and anticancer effects of ChitosanNPs-EO than the AlginateNPs-EO and EO. It could thus be considered for in vivo studies.

Author Contribution EZ interpreted ATR-FTIR and cooperated in drafting with MO. MHA performed antifungal assays. HA wrote a discussion and literature review. FY performed antibacterial assays. HM prepared nanoparticles. HEK revised the MS. MO design of study, analysis, and drafted the MS. All authors contributed to drafting and approving the final MS.

Funding Fasa University of Medical Sciences supported this study grant No. 402004.

Data Availability All data are available by reasonable request from the corresponding author.

Declarations

Informed Consent None.

Consent for Publication Not applicable.

Research Involving Humans and Animals Statement This study has been ethically approved (IR.FUMS.REC.1402.033).

Conflict of Interest The authors declare no competing interests.

References

1. Jamshidi-Kia, F., Lorigooini, Z., & Amini-Khoei, H. (2018). Medicinal plants: Past history and future perspective. *J HerbMed Pharmacol*, *7*(1), 1–7. https://doi.org/10.15171/jhp.2018.01.
2. Balunas, M. J., & Kinghorn, A. D. (2005). Drug discovery from medicinal plants. *Life Sciences*, *78*(5), 431–441. https://doi.org/10.1016/j.lfs.2005.09.012.
3. Han, Y. A., Song, C. W., Koh, W. S., Yon, G. H., Kim, Y. S., Ryu, S. Y., Kwon, H. J., & Lee, K. H. (2013). Anti-inflammatory effects of the Zingiber officinale roscoe constituent 12-dehydrogingerdione in lipopolysaccharide-stimulated raw 264.7 cells.

Phytotherapy Research: Ptr, *27*(8), 1200–1205. https://doi.org/10.1002/ptr.4847.
4. Osanloo, M., Ghanbariasad, A., & Taghinezhad, A. (2022). Antioxidant and anticancer activities of Anethum graveolens L., Citrus limon (L.) Osbeck and Zingiber officinale Roscoe essential oils. *Tradit Integr Med, 6*(4), 333–347. https://doi.org/10.18502/tim.v6i4.8266
5. Stoner, G. D. (2013). Ginger: Is it ready for prime time? *Cancer Prevention Research (Philadelphia, Pa.)*, *6*(4), 257–262. 10.1158/1940–6207.CAPR-13-0055.
6. Zhang, M., Viennois, E., Prasad, M., Zhang, Y., Wang, L., Zhang, Z., Han, M. K., Xiao, B., Xu, C., & Srinivasan, S. (2016). Edible ginger-derived nanoparticles: A novel therapeutic approach for the prevention and treatment of inflammatory bowel disease and colitis-associated cancer. *Biomaterials*, *101*, 321–340. https://doi.org/10.1016/j.biomaterials.2016.06.018.
7. Kumar, N. V., Murthy, P. S., Manjunatha, J. R., & Bettadaiah, B. (2014). Synthesis and quorum sensing inhibitory activity of key phenolic compounds of ginger and their derivatives. *Food Chemistry*, *159*, 451–457. https://doi.org/10.1016/j.foodchem.2014.03.039.
8. Wei, C. K., Tsai, Y. H., Korinek, M., Hung, P. H., El-Shazly, M., Cheng, Y. B., Wu, Y. C., Hsieh, T. J., & Chang, F. R. (2017). 6-Paradol and 6-shogaol, the pungent compounds of ginger, promote glucose utilization in adipocytes and myotubes, and 6-paradol reduces blood glucose in high-fat diet-fed mice. *International Journal of Molecular Sciences, 18*(1), 168. https://doi.org/10.3390/ijms18010168
9. Chakotiya, A. S., Tanwar, A., Narula, A., & Sharma, R. K. (2017). Zingiber officinale: Its antibacterial activity on Pseudomonas aeruginosa and mode of action evaluated by flow cytometry. *Microbial Pathogenesis*, *107*, 254–260. https://doi.org/10.1016/j.micpath.2017.03.029.
10. Kim, H-S., & Park, H-D. (2013). Ginger extract inhibits biofilm formation by Pseudomonas aeruginosa PA14. *PLoS One*, *8*(9), e76106. https://doi.org/10.1371/journal.pone.0076106.
11. Michel-Briand, Y., & Baysse, C. (2002). The pyocins of Pseudomonas aeruginosa. *Biochimie*, *84*(5–6), 499–510. https://doi.org/10.1016/s0300-9084(02)01422-0.
12. Sebiomo, A., Awofodu, A., Awosanya, A., Awotona, F., & Ajayi, A. (2011). Comparative studies of antibacterial effect of some antibiotics and ginger (Zingiber officinale) on two pathogenic bacteria. *J Microbiol Antimicrob*, *3*(1), 18–22. https://doi.org/10.5897/JMA.9000027.
13. Rampogu, S., Baek, A., Gajula, R. G., Zeb, A., Bavi, R. S., Kumar, R., Kim, Y., Kwon, Y. J., & Lee, K. W. (2018). Ginger (Zingiber officinale) phytochemicals-gingerenone-A and shogaol inhibit SaHPPK: molecular docking, molecular dynamics simulations and in vitro approaches. *Annals of Clinical Microbiology and Antimicrobials, 17*(1), 16. https://doi.org/10.1186/s12941-018-0266-9
14. Manolakaki, D., Velmahos, G., Kourkoumpetis, T., Chang, Y., Alam, H. B., De Moya, M. M., & Mylonakis, E. (2010). Candida infection and colonization among trauma patients. *Virulence*, *1*(5), 367–375. https://doi.org/10.4161/viru.1.5.12796.
15. Brandt, M. E., & Lockhart, S. R. (2012). Recent taxonomic developments with Candida and other opportunistic yeasts. *Curr Fungal Infect Rep*, *6*(3), 170–177. https://doi.org/10.1007/s12281-012-0094-x.
16. Shokohi, T., Moradi, N., Badram, L., Badali, H., Ataollahi, M. R., & Afsarian, M. H. (2018). Molecular identification of clinically common and uncommon yeast species. *Jundishapur J Microbiol*, *11*(10), e66240. https://doi.org/10.5812/jjm.66240.
17. Azizi, Z., Omran, S. M., Sheikhzadeh, S., Gholinia, H., & Gharekhani, S. (2023). Antifungal effect of ginger essential oil spray on Candida albicans adhering to self-cure acrylic plates. *Front dent, 20*, 3. https://doi.org/10.18502/fid.v20i3.12279
18. Atai, Z., Atapour, M., & Mohseni, M. (2009). Inhibitory effect of ginger extract on Candida albicans. *Am J Appl Sci*, *6*(6), 1067–1069.
19. Saha, A., Blando, J., Silver, E., Beltran, L., Sessler, J., & DiGiovanni, J. (2014). 6-Shogaol from dried ginger inhibits growth of prostate cancer cells both in vitro and in vivo through inhibition of STAT3 and NF-κB signaling. *Cancer Prevention Research (Philadelphia, Pa.)*, *7*(6), 627–638. https://doi.org/10.1158/1940-6207.CAPR-13-0420.
20. El-Ashmawy, N. E., Khedr, N. F., El-Bahrawy, H. A., & Abo Mansour, H. E. (2018). Ginger extract adjuvant to doxorubicin in mammary carcinoma: Study of some molecular mechanisms. *European Journal of Nutrition*, *57*, 981–989. https://doi.org/10.1007/s00394-017-1382-6.
21. WHO Breast cancer 2023 [cited Des. 2023]. https://www.who.int/news-room/fact-sheets/detail/breast-cancer.
22. Dupuis, V., Cerbu, C., Witkowski, L., Potarniche, A. V., Timar, M. C., Żychska, M., & Sabliov, C. M. (2022). Nanodelivery of essential oils as efficient tools against antimicrobial resistance: A review of the type and physical-chemical properties of the delivery systems and applications. *Drug Delivery*, *29*(1), 1007–1024. https://doi.org/10.1080/10717544.2022.2056663.
23. O Elzoghby, A., Abd-Elwakil, M., Abd-Elsalam, M., T Elsayed, K., Hashem, M., & Mohamed, Y. O (2016). Natural polymeric nanoparticles for brain-targeting: Implications on drug and gene delivery. *Curr Pharm Des*, *22*(22), 3305–3323. https://doi.org/10.2174/1381612822666160204120829.
24. Detsi, A., Kavetsou, E., Kostopoulou, I., Pitterou, I., Pontillo, A. R. N., Tzani, A., Christodoulou, P., Siliachli, A., & Zoumpoulakis, P. (2020). Nanosystems for the encapsulation of natural products: The case of chitosan biopolymer as a matrix. *Pharmaceutics*, *12*(7), 669. https://doi.org/10.3390/pharmaceutics12070669.
25. Rahmani, H., Ghanbariasad, A., Meshkibaf, M. H., Molazade, A., Heiran, R., Safari, M., & Osanloo, M. (2023). Chitosan nanoparticles containing α-pinene and Rosmarinus officinalis L. essential oil: Effects on human melanoma cells' viability and expression of apoptosis-involved genes. *Polymer Bulletin*. https://doi.org/10.1007/s00289-023-04839-w.
26. Valizadeh, A., Hosseinzadeh, M., Heiran, R., Hatami, S., Hosseinipour, A., & Osanloo, M. (2023). Alginate nanoparticles containing Lavandula angustifolia essential oil as a potential potent, biocompatible and low-cost antitumor agent. *Polymer Bulletin*. https://doi.org/10.1007/s00289-023-04797-3.
27. Clinical and Laboratory Standards Institute (CLSI). (2008). *Reference method for broth dilution antifungal susceptibility testing of yeasts; approved standard-third edition, M27–A3*. CLSI.
28. Clinical and Laboratory Standards Institute (CLSI). (2012). *Reference method for broth dilution antifungal susceptibility testing of yeasts: Fourth informational supplement M27-S4*. CLSI.
29. Osanloo, M., Ghaznavi, G., & Abdollahi, A. (2020). Sureveying the chemical composition and antibacterial activity of essential oils from selected medicinal plants against human pathogens. *Iran J Microbiol*, *12*(6), 505–512. https://doi.org/10.18502/ijm.v12i6.5032.
30. Roozitalab, G., Yousefpoor, Y., Abdollahi, A., Safari, M., Rasti, F., & Osanloo, M. (2022). Antioxidative, anticancer, and antibacterial activities of a nanoemulsion-based gel containing Myrtus communis L. essential oil. *Chemical Papers*, *76*(7), 4261–4271. https://doi.org/10.1007/s11696-022-02185-1.
31. Barry, A. L., Pfaller, M. A., Brown, S. D., Espinel-Ingroff, A., Ghannoum, M. A., Knapp, C., Rennie, R. P., Rex, J. H., & Rinaldi, M. G. (2000). Quality control limits for broth microdilution susceptibility tests of ten antifungal agents. *Journal of Clinical*

Microbiology, *38*(9), 3457–3459. https://doi.org/10.1128/JCM.38.9.3457-3459.2000.
32. Blowman, K., Magalhaes, M., Lemos, M. F. L., Cabral, C., & Pires, I. M. (2018). Anticancer properties of essential oils and other natural products. *Evid Based Complement Alternat Med, 2018*, 3149362. https://doi.org/10.1155/2018/3149362
33. Osanloo, M., Yousefpoor, Y., Alipanah, H., Ghanbariasad, A., Jalilvand, M., & Amani, A. (2022). In-vitro assessment of essential oils as anticancer therapeutic agents: A systematic literature review. *Jordan J Pharm Sci, 15*(2), 173–203. https://doi.org/10.35516/jjps.v15i2.319
34. Sehgal, I. S., Choudhary, H., Dhooria, S., Aggarwal, A. N., Bansal, S., Garg, M., Behera, D., Chakrabarti, A., & Agarwal, R. (2019). Prevalence of sensitization to aspergillus flavus in patients with allergic bronchopulmonary aspergillosis. *Medical Mycology*, *57*(3), 270–276. https://doi.org/10.1093/mmy/myy012.
35. Aslani, N., Shokohi, T., Ataollahi, M. R., Ansari, S., Gholampour, Y., Khani Jeihooni, A., & Afsarian, M. H. (2019). In vitro activity of four triazole antifungal drugs against clinically common and uncommon yeast species. *Curr Med Mycol*, *5*(4), 14–19. https://doi.org/10.18502/cmm.5.4.1949.
36. Aslani, N., Kokabi, R., Moradi, F., Abbasi, K., Vaseghi, N., & Afsarian, M. H. (2021). Characterization of Candida species isolated from vulvovaginal candidiasis by MALDI-TOF with in vitro antifungal susceptibility profiles. *Curr Med Mycol*, *7*(4), 6–11. https://doi.org/10.18502/cmm.7.4.8405.
37. Gomez-Gaviria, M., Ramirez-Sotelo, U., & Mora-Montes, H. M. (2022). Non-albicans Candida species: Immune response, evasion mechanisms, and new plant-derived alternative therapies. *J Fungi, 9*(1). https://doi.org/10.3390/jof9010011
38. Papadimitriou-Olivgeris, M., Spiliopoulou, A., Kolonitsiou, F., Bartzavali, C., Lambropoulou, A., Xaplanteri, P., Anastassiou, E. D., Marangos, M., Spiliopoulou, I., & Christofidou, M. (2019). Increasing incidence of candidaemia and shifting epidemiology in favor of Candida non-albicans in a 9-year period (2009–2017) in a university Greek hospital. *Infection*, *47*(2), 209–216. https://doi.org/10.1007/s15010-018-1217-2.
39. Rajeswari, M. R., Hanumanthappa, A. R., Kalyani, M., & Vijayaraghavan, R. (2018). Distribution and antifungal susceptibility profile of Candida species from candiduria cases at a tertiary care hospital. *Int J Res Pharm Sci*, *9*(3), 700–705. https://doi.org/10.26452/ijrps.v9i3.1550.
40. Franconi, I., Rizzato, C., Tavanti, A., Falcone, M., & Lupetti, A. (2023). Paradigm shift: Candida parapsilosis sensu stricto as the most prevalent Candida species isolated from bloodstream infections with increasing azole-non-susceptibility rates: Trends from 2015–2022 survey. *J Fungi*, *9*(10). https://doi.org/10.3390/jof9101012.
41. Mamali, V., Siopi, M., Charpantidis, S., Samonis, G., Tsakris, A., & Vrioni, G. (2022). Increasing incidence and shifting epidemiology of candidemia in Greece: Results from the first nationwide 10-year survey. *J Fungi*, *8*(2). https://doi.org/10.3390/jof8020116.
42. Zhang, W., Zhan, M., Wang, N., Fan, J., Han, X., Li, C., Liu, J., Li, J., Hou, Y., Wang, X., et al. (2023). In vitro susceptibility profiles of Candida parapsilosis species complex subtypes from deep infections to nine antifungal drugs. *Journal of Medical Microbiology*, *72*(3). https://doi.org/10.1099/jmm.0.001640.
43. Wu, Y. M., Huang, P. Y., Lu, J. J., Shie, S. S., Ye, J., Wu, T. S., & Huang, C. T. (2018). Risk factors and outcomes of candidemia caused by Candida parapsilosis complex in a medical center in northern Taiwan. *Diagnostic Microbiology and Infectious Disease*, *90*(1), 44–49. https://doi.org/10.1016/j.diagmicrobio.2017.10.002.
44. Nerilo, S. B., Rocha, G. H. O., Tomoike, C., Mossini, S. A., Grespan, R., Mikcha, J. M., & MachinskiJr, M. (2016). Antifungal properties and inhibitory effects upon aflatoxin production by Zingiber officinale essential oil in aspergillus flavus. *International Journal of Food Science & Technology*, *51*(2), 286–292. https://doi.org/10.1111/ijfs.12950.
45. Nerilo, S. B., Romoli, J. C. Z., Nakasugi, L. P., Zampieri, N. S., Mossini, S. A. G., Rocha, G. H. O., Gloria EMd, A. F., & BAd, MachinskiJr, M. (2020). Antifungal activity and inhibition of aflatoxins production by Zingiber officinale Roscoe essential oil against aspergillus flavus in stored maize grains. *Ciência Rural*, *50*(6), e20190779. https://doi.org/10.1590/0103-8478cr20190779.
46. Singh, P. P., Jaiswal, A. K., Kumar, A., Gupta, V., & Prakash, B. (2021). Untangling the multi-regime molecular mechanism of verbenol-chemotype Zingiber officinale essential oil against aspergillus flavus and aflatoxin B1. *Scientific Reports*, *11*(1), 6832. https://doi.org/10.1038/s41598-021-86253-8.
47. Moon, Y-S., Lee, H-S., & Lee, S-E. (2018). Inhibitory effects of three monoterpenes from ginger essential oil on growth and aflatoxin production of aspergillus flavus and their gene regulation in aflatoxin biosynthesis. *Appl Biol Chem*, *61*, 243–250. https://doi.org/10.1007/s13765-018-0352-x.
48. Aghazadeh, M., Zahedi Bialvaei, A., Aghazadeh, M., Kabiri, F., Saliani, N., Yousefi, M., Eslami, H., & Samadi Kafil, H. (2016). Survey of the antibiofilm and antimicrobial effects of Zingiber officinale (in vitro study). *Jundishapur J Microbiol, 9*(2), e30167. https://doi.org/10.5812/jjm.30167
49. Mohammadi, R., & Moattar, F. (2007). Antifungal activity of Zingiber officinale Rosc. essential oil against fluconazole resistant vaginal isolates of Candida albicans. *J Medicinal Plants, 6*(24), 22–27.
50. Mostafa, A. A., & Amer, S. M. (2013). Molecular characterization of toxigenic aspergillus flavus strains isolates from animal feed stuff in Egypt. *Life Sci J*, *10*(2), 1102–1109.
51. Abd-Elsalam, K. A., Alghuthaymi, M. A., Shami, A., Rubina, M. S., Abramchuk, S. S., Shtykova, E. V., & Yu. Vasil'kov, A. (2020). Copper-chitosan nanocomposite hydrogels against aflatoxigenic Aspergillus flavus from dairy cattle feed. *J Fungi, 6*(3), 112. https://doi.org/10.3390/jof6030112
52. Yien, L., Zin, N. M., Sarwar, A., & Katas, H. (2012). Antifungal activity of chitosan nanoparticles and correlation with their physical properties. *Int J Biomater*, *2012*, 632698. https://doi.org/10.1155/2012/632698.
53. Spadari, C. C., Lopes, L. B., & Ishida, K. (2017). Potential use of alginate-based carriers as antifungal delivery system. *Frontiers in Microbiology*, *8*, 97. https://doi.org/10.3389/fmicb.2017.00097.
54. Hosseini, S. M., Hosseini, H., Mohammadifar, M. A., Mortazavian, A. M., Mohammadi, A., Khosravi-Darani, K., Shojaee-Aliabadi, S., Dehghan, S., & Khaksar, R. (2013). Incorporation of essential oil in alginate microparticles by multiple emulsion/ionic gelation process. *International Journal of Biological Macromolecules*, *62*, 582–588. https://doi.org/10.1016/j.ijbiomac.2013.09.054.
55. Soliman, E. A., El-Moghazy, A. Y., El-Din, M. M., & Massoud, M. A. (2013). Microencapsulation of essential oils within alginate: Formulation and in vitro evaluation of antifungal activity. *J Encapsulation Adsorpt sci*, *13*(1), 48–55. https://doi.org/10.4236/jeas.2013.31006.
56. Hadidi, M., Pouramin, S., Adinepour, F., Haghani, S., & Jafari, S. M. (2020). Chitosan nanoparticles loaded with clove essential oil: Characterization, antioxidant and antibacterial activities. *Carbohydrate Polymers*, *236*, 116075. https://doi.org/10.1016/j.carbpol.2020.116075.
57. Burt, S. (2004). Essential oils: Their antibacterial properties and potential applications in foods—A review. *International Journal of Food Microbiology, 94*(3), 223–253. https://doi.org/10.1016/j.ijfoodmicro.2004.03.022

58. Chandrasekaran, M., Kim, K. D., & Chun, S. C. (2020). Antibacterial activity of chitosan nanoparticles: A review. *Processes*, *8*(9), 1173. https://doi.org/10.3390/pr8091173.
59. Seshadri, V. D., Oyouni, A. A. A., Bawazir, W. M., Alsagaby, S. A., Alsharif, K. F., Albrakati, A., & Al-Amer, O. M. (2022). Zingiberene exerts chemopreventive activity against 7, 12-dimethylbenz (a) anthracene-induced breast cancer in Sprague-Dawley rats. *Journal of Biochemical and Molecular Toxicology*, *36*(10), e23146. https://doi.org/10.1002/jbt.23146.
60. Chen, H., Tang, X., Liu, T., Jing, L., & Wu, J. (2019). Zingiberene inhibits in vitro and in vivo human colon cancer cell growth via autophagy induction, suppression of PI3K/AKT/mTOR pathway and caspase 2 deactivation. *Journal of B.U.On. : Official Journal of the Balkan Union of Oncology*, *24*(4), 1470–1475. PMID: 31646793.
61. Noufal, Z. M., Gayathri, R., & Priya, V. V. (2019). Influence of zingiberene on the biofilm formation of Streptococcus mutans. *Drug Invent Today*, *12*(6), 1261–1263.
62. Yousefi, M., Mohammadi, V. G., Shadnoush, M., Khorshidian, N., & Mortazavian, A. M. (2022). Zingiber officinale essential oil-loaded chitosan-tripolyphosphate nanoparticles: Fabrication, characterization and in-vitro antioxidant and antibacterial activities. *Food Science and Technology International*, *28*(7), 592–602. https://doi.org/10.1177/10820132211040917.
63. Khayatzadeh, J., Es-haghi, A., & Shadan, B. (2022). Anti-cancer effects of nanoemulsion prepared using Zingiber officinale L. tincture against PC3 prostate cancer cells. *Nanomed J, 9*(3), 241–251. https://doi.org/10.22038/NMJ.2022.64734.1676
64. Salehi, F., Behboudi, H., Kavoosi, G., & Ardestani, S. K. (2020). Incorporation of Zataria multiflora essential oil into chitosan biopolymer nanoparticles: A nanoemulsion based delivery system to improve the in-vitro efficacy, stability and anticancer activity of ZEO against breast cancer cells. *International Journal of Biological Macromolecules*, *143*, 382–392. https://doi.org/10.1016/j.ijbiomac.2019.12.058.
65. Soltani, M., Etminan, A., Rahmati, A., Behjati Moghadam, M., Ghaderi Segonbad, G., & Homayouni Tabrizi, M. (2022). Incorporation of Boswellia sacra essential oil into chitosan/TPP nanoparticles towards improved therapeutic efficiency. *Materials Technology*, *37*(11), 1703–1715. https://doi.org/10.1080/10667857.2021.1976364.
66. Yarian, F., Yousefpoor, Y., Hatami, S., Zarenezhad, E., Peisepar, E., Alipanah, H., & Osanloo, M. (2023). Comparison effects of alginate nanoparticles containing Syzygium aromaticum essential oil and eugenol on apoptotic regulator genes and viability of A-375 and MCF-7 cancer cell lines. *BioNanoScience, 13*, 911–919. https://doi.org/10.1007/s12668-023-01121-1